

## The College at Brockport: State University of New York Digital Commons @Brockport

---

Senior Honors Theses

Master's Theses and Honors Projects

---

5-15-2014

# Disruption of Caveolae Lipid Rafts and the Effects on Melanin-concentrating Hormone Receptor-1 Localization: A Pharmacological Study

Colin King

*The College at Brockport*, [cking354@gmail.com](mailto:cking354@gmail.com)

Follow this and additional works at: <http://digitalcommons.brockport.edu/honors>

 Part of the [Biology Commons](#), and the [Pharmacology Commons](#)

---

### Repository Citation

King, Colin, "Disruption of Caveolae Lipid Rafts and the Effects on Melanin-concentrating Hormone Receptor-1 Localization: A Pharmacological Study" (2014). *Senior Honors Theses*. 56.

<http://digitalcommons.brockport.edu/honors/56>

This Honors Thesis is brought to you for free and open access by the Master's Theses and Honors Projects at Digital Commons @Brockport. It has been accepted for inclusion in Senior Honors Theses by an authorized administrator of Digital Commons @Brockport. For more information, please contact [kmyers@brockport.edu](mailto:kmyers@brockport.edu).

Disruption of Caveolae Lipid Rafts and the Effects on Melanin-concentrating  
Hormone Receptor-1 Localization: A Pharmacological Study

---

A Senior Honor Thesis

Submitted in Partial Fulfillment of the Requirements  
for Graduation in the Honors College

By  
Colin King  
Biology Major  
The College at Brockport  
May 15, 2014

Thesis Director: Dr. Laurie B. Cook, Associate Professor, Biological Sciences

## **ABSTRACT**

Melanin-concentrating hormone (MCH) is integral to the regulation of human appetite. MCH targets G protein-coupled receptors in the brain and peripheral tissues. When MCH receptor 1 binds MCH on the surface of cells, it activates multiple signaling pathways, then desensitizes. Internalization of MCH-bound MCHR1 is only thought to be partially responsible for the loss of MCH signaling capacity of cells. Previous research has shown that MCH receptors are enriched in caveolae and specifically complex with caveolin-1. Caveolin-1 is a key structural component of caveolae, which are cholesterol-based lipid rafts that are known for concentrating signaling molecules and clathrin-independent endocytosis. This study aims to investigate how MCH signaling would be affected if MCH receptors weren't enriched in these regions. Pharmacological treatments were used to achieve this goal as caveolae formation was disrupted with the antibiotic nystatin, a cholesterol inhibitor. It has been shown that sodium carbonate-based extraction procedure followed by flotation on sucrose density centrifugation isolates caveolae from other cell contents. Caveolae-isolation procedures to detect caveolin-1 were undertaken to indicate that untreated BHK-570 cells contained caveolin-1 in fractions 4 and 5 of the sucrose gradients while a gradient shift of caveolin-1 to fractions 7-10 in nystatin-treated cells occurred. Such shift confirmed that there was a partial disruption of caveolae within the treated cells. Future experiments will test whether other pharmacological inhibitors such as filipin and methyl- $\beta$ -cyclodextrin as well as caveolin-1 RNAi are better able to deplete caveolae from cells as well as their impact on MCH signaling.

## **INTRODUCTION**

### **Obesity**

Obesity is caused by an accumulation of adipose tissue resulting in the impairment of one's health. It is estimated that incidences and diseases such as strokes, coronary artery disease, and type II diabetes have increased over the past decade in America due to the rise in the prevalence of obesity. To be considered obese a person must have a body mass index (BMI) of  $\geq 30$  (Vemmos et al. 2011). Currently, one-third of Americans have a BMI above this number and experience numerous acute and chronic problems and an attenuation of life expectancy (Kopelman 2000).

Obesity in America is becoming so prevalent that it is reaching epidemic proportions. By 2030 it is estimated that 42% of adult Americans will fit the criteria for being obese (Ogden et al. 2014). A 10% increase in incidence over the next 15 years will continue to place a heavy burden on the lives of those afflicted with obesity and the healthcare system as a whole. With more of the population living unhealthy lives, doctors will begin to see an increase in obesity-related problems that will strain the funds of the United States healthcare system (Finkelstein et al. 2009).

The estimated annual medical cost of obesity in the United States was \$147 billion in 2008. Furthermore, the medical costs for people who are obese were \$1,429 higher than those of normal weight per year. These costs accrue because of a higher use of services and medical treatments that were aimed at reducing the adverse affects of obesity either with surgical procedures or pharmacological treatments (Finkelstein et al. 2009). It is the hope that with implementation of the Affordable Health Care Act, there will be broad access to primary medical

services and educational material that will act as preventative measures to begin to reduce both the financial and personal cost of obesity (Finkelstein et al. 2009; Derksen 2013).

A challenge with reducing obesity is the numerous facets of the disease. There is a strong correlation between obesity and genetics; however environmental factors can also impact an individual. The family, culture, and ethnicity that a person belongs too can directly affect how a person interacts with food and energy expenditure. For instance, cultures that emphasize large meals and embrace a sedentary lifestyle may be more prone to obesity-related diseases (Kopelman 2000). Non-Hispanic blacks have the highest age-adjusted rates of obesity (47.8%) followed by Hispanics (42.5%), non-Hispanic whites (32.6%), and non-Hispanic Asians (10.8%) while obesity is higher among middle-aged adults, 40-59 years old (39.5%) than among younger adults, age 20-39 (30.3%) or adults over 60 or above (35.4%) adults (Finkelstein et al. 2009). Obesity results from an imbalance in energy intake but the cause of that imbalance must be addressed in order to combat this epidemic.

### **Regulation of Food Intake**

Food consumption is regulated within the human body by neurotransmitters, signaling peptides, and feedback loops that allow the body to either potentiate satiety or hunger signals. When the body experiences a state of fasting or ingestion, the brain is able to determine its nutritional state through signals from the liver, gastrointestinal tract (GIT), pancreas and adipose tissue. Other interpretations made by the brain concerning the energy needs of the body are carried out by hormones such as leptin and ghrelin (Williams, Harrold, and Cutler, 2000; Woods et al. 1998).

The hypothalamus and the brain stem are the main centers of the brain associated with food intake. The afferent nerves associated with the liver, Gastro Intestinal Tract, pancreas and

adipose tissue are integrated with the hypothalamus and other higher ordered brain systems that control reward and learning behavior. The arcuate nucleus (ARC) of the hypothalamus drives both fasting and feeding within the body. Orexigenic neurons present in the ARC express neuropeptide Y (NPY) and agouti-related protein both of which potentiate feeding signals. The ARC also contains anorexigenic neurons that decrease feeding behavior by releasing alpha-melanocyte stimulating hormone. ARC also plays a role in paraventricular nuclei stimulation within the hypothalamus, whose purpose is to regulate energy expenditure (Sam et al. 2012).

Food consumption is not only controlled through neural signals, but certain hormones within the endocrine system have been shown to influence energy homeostasis through negative feedback loops containing leptin, melanin-concentrating hormone (MCH), and ghrelin. Peripheral signals from leptin inhibit NPY-releasing neurons within the hypothalamus that leads to a reduction in MCH release from the hypothalamus. A decrease in MCH secretion allows appetite signals to potentiate, effectively leading to food intake. Nevertheless, the reverse of this process elicits satiety mechanisms, indicating that as leptin signaling decreases MCH signaling increases, resulting in the formation of cyclical feeding patterns (Sam et al. 2012).

Like its counterpart leptin, ghrelin is a natural ligand of growth hormone that is secreted by D cells within the fundus of the stomach to increase food intake and promote weight gain. After a person has ingested a meal, ghrelin can facilitate gastric emptying, but as excess adipose tissue becomes present, ghrelin secretions begin to decrease to prevent overfeeding. This feedback mechanism allows the GI tract to both promote and prohibit the feelings of starvation and satiety controlled by the hypothalamus (Delporte 2012).

For those who are morbidly obese, there are numerous factors beyond food intake that regulate their daily meals. It has become increasingly clear that obesity is hard to combat due to

the metabolic changes that adipose tissue can inflict on an obese individual. Within the body adipose tissue is responsible for the release of adipokines that interact with energy homeostasis. Hardwood and colleagues report leptin secretion via excess adipose tissue begins to increase food intake and the silencing of satiety signals. As a result, obesity is a disease that can be self sustained and extremely hard to combat (Harwood 2012).

### **Melanin-concentrating Hormone**

Melanin-concentrating hormone (MCH) was discovered in teleost fish where it functions to lighten its scales. In mammals, MCH is a highly conserved neuropeptide that is orexigenic within the hypothalamus and increases hunger sensations (Pissios and Maratos-Flier 2003). MCH also controls other physiological effects such as sleep-wake cycles, voiding behaviors and depression (Hassani, Lee, and Jones 2009). In addition to neurological effects, MCH can also act upon peripheral tissues such as adipocytes. An increase in leptin mRNA transcription is seen with elevated levels of MCH further supporting the cyclic nature of these two metabolic hormones (Bradley et al. 2000).

### **Melanin-concentrating Hormone Receptor-1**

In order to affect adipocytes, MCH must first bind to membrane receptors on targeted cells. MCH lacks the ability to simply diffuse through the membrane so it must first bind to melanin-concentrating hormone receptor-1 (MCHR-1). MCHR-1 is a G protein-coupled receptor (GPCR) that is capable of binding several different heterotrimeric proteins including  $G_{i/o}$  and  $G_q$  allowing for diverse signaling pathways (Gehlert et al. 2009).

Secondary signaling pathways activated by MCHR-1 include activation of the extracellular-signal-regulated kinase (ERK) pathway and the mitogen-activated protein kinase 1 pathway (MAPK1). Both ERK and MAPK1 pathways lead to an increase in transcription factors

within neural cells, enhancing the MCH signal. In addition, MCH can increase the amount of intracellular free  $\text{Ca}^{2+}$  that promotes cell growth, proliferation, and gene transcription (Pissios and Maratos-Flier 2003).

MCH also affects peripheral tissues such as adipocytes. Bradley and colleagues report that 3T3L-1 express MCHR-1 that can bind MCH and activate the ERK pathway. ERK activation leads to an increase in adipocyte secretion of leptin, a prominent satiety signal. Consequently, leptin expression is up regulated as a result of MCH-MCHR-1 interaction indicating a potentially viable target for obesity treatments (Bradley et al. 2000).

A challenge in targeting secondary signaling of MCH is the identification of the internalization pathway that the MCH-MCHR-1 complex uses. Saito and colleagues investigated the possibility of MCHR-1 internalization via clathrin coated vesicles and found that after inhibition, only 66% of receptors were not internalizing. These results suggest that non-clathrin-mediated endocytosis was occurring (Saito, Hamamoto, and Kobayashi 2013). Consequently, there may be other mechanisms and areas along the plasma membrane that control MCH-MCHR-1 internalization.

### **Lipid Rafts**

MCHR-1, along with many other transmembrane receptors, is associated with cholesterol and lipid-enriched portions of the plasma membrane of the cell. These areas are described as lipid rafts which consist of dynamic assemblies of cholesterol and sphingolipids. Lipid rafts are highly hydrophobic areas dispersed throughout the plasma membrane. Both neurons and adipocytes have been shown to contain MCHR-1 and other receptors that co localize with lipid rafts enhancing signal amplification (Simons 2001; Cook, Delorme-Axford, and Robinson 2008).



Previous studies have shown that MCHR-1 co localizes specifically with a subset of lipid rafts known as caveolae. Caveolae are invaginations found on the cell surface and are indicated by lipid enriched regions and the presence of caveolin-1, an integral membrane protein that tightly binds cholesterol (Cook *et al.* 2008). It is speculated that caveolae interacts with MCHR-1 in two ways. First, caveolae can organize signaling molecules such as MCHR-1, increasing the signal generated from MCH binding via signal amplification. Second, caveolae is integral to the internalization of these membrane receptors. As a result, MCH/MCHR-1 internalization is carried out through the endocytotic pathway where a portion of caveolae will be removed from the plasma membrane and arrive in the cytoplasm as an early endosome that can potentiate secondary pathways such as the ERK and MAPK1 leading to cellular desensitization (Simons 2001; Cook *et al.* 2008).

Speculation surrounds this pathway as research continues to show that cellular desensitization continues despite the lack of caveolae. Moden and colleagues report that clathrin-mediated endocytosis may be the primary cause of MCH/MCHR-1 internalization. Clathrin-mediated endocytosis refers the coating and internalization of a receptor protein complex via clathrin, a protein that is involved in vesicle coating. After 30 minutes of MCH exposure, a 44% reduction in the initial surface levels of MCHR-1 was observed. Reduction of cell surface MCHR-1 indicates the presence of internalization via a clathrin mediated endocytotic pathway (Moden et al. 2013).

Once the MCH/MCHR-1 complex is internalized either by clathrin or caveolae mediated endocytosis, receptors can be degraded or recycled back to the plasma membrane. Because MCH/MCHR-1 internalization halts secondary messengers, this process is labeled as

homologous desensitization in which a receptor activation-independent pathway is mediated through the effects of the secondary messengers it activates. (Ferguson 2001).

### **Specific Aims**

With the increasing prevalence of obesity in the United States and around the world, there is a need for targeted treatments that will be able to reduce this epidemic. The effort to end obesity is currently being supported by educational outreach programs and health care administrators that warn against the dangers of cardiovascular disease and type II diabetes.

There is promise however, in targeting MCH signaling through MCHR-1 in efforts to treat obesity. Past studies have shown that MCHR-1 knockout mice have shown an increase in adipose tissue. When knockout occurs, there is a decrease in the satiety signals leading to increased caloric intake. As a result, MCH agonist studies have shown that satiety signals will indeed increase and lead to a lean body phenotype (Bjursell 2006).

Despite these past endeavors little is still known about the desensitization mechanisms of MCHR-1 and how its co localization with caveole affects MCH internalization. Therefore it was the purpose of this to present information on the relationship between caveolae and MCH internalization to indicate whether caveolae internalization is important in MCH signaling. In order to accomplish this task, three specific aims were undertaken.

#### *Specific Aim 1*

Engaging in meaningful research in a lab requires a mastery of certain types of techniques. For this research to be successful, correct procedures need to be carried out, in particular the generation of a sucrose gradient and western blot analysis. A sucrose gradient is imperative to this research because it will allow for the separation of cellular components based upon their molecular weight. By creating a useable sucrose gradient caveolae isolation

procedures could be carried out that would separate the contents of the cell based upon density. Once a successful sucrose gradient was produced, the process of western blotting was carried out. Western blotting was used in order to isolate and quantify the caveole present within the harvested cells. The intricate steps required to achieve a viable western blot were perfected over time and ultimately led to data that could be interpreted.

#### *Specific Aim #2*

After the techniques needed to illustrate the presence of caveolae, procedures were carried out that were aimed at disrupting the formation of caveolae within the plasma membrane. The disruption was accomplished using antibiotics, nystatin which is a well known cholesterol inhibitor. Overall, our specific aim was directed towards demonstrating the efficacy of nystatin treatments on the disruption of caveolae.

#### *Specific Aim #3*

Disruption of caveole determined by nystatin treatments would only be applicable to our research if an interruption in MCH –MCHR-1 occurs. This disruption of signaling was tested through the administration of MCH to cells pretreated with Nystatin. Subsequent tests indicated if MCH-MCHR-1 were internalized via the caveolae pathway or if disruption of these lipid rafts truly hindered signal transduction. Depletion of caveolae and MCH treatments were the most reliable way to show if MCHR-1 co localization with caveolae is a future treatment target.

Nonetheless, Understanding the relationship between caveolae, MCHR-1 and MCH internalization could enhance the knowledge of the mechanism of MCH/MCHR-1 desensitization and lead to a viable treatment option that can combat the heavy burden of obesity.

## **MATERIALS/METHODS**

### **Tissue Culture**

BHK-570 cells (ATCC) were cultured as a tissue monolayer using DMEM<sup>-</sup> media (CellGro) containing 10% fetal bovine serum (FBS) (Atlanta Biological). Cells were fed every five days and passaged when they were confluent. Cells were passaged by the addition of new media into a culture flask and transfer of cells after the use of trypsin, a serum protease that detaches the cells from the old flask. Culture conditions throughout cell proliferation and passage were set at 37° C, 5% CO<sub>2</sub>, and 90% humidity.

### **Transfection**

Cell lines were transfected at 90% confluency in 10cm culture dishes. Transfections were carried out following the recommended protocol from SigmaGen utilizing 15 µL of their LipoD293 reagent and 5 µg of VSVg MCHR-1 plasmid. Media was changed 1 hour pre-transfection and experiments were run approximately 72 hours post transfection.

### **Expansion of Transfection**

Once cells within a 10cm dish were 90% confluent and transfected, media was aspirated off and cells were transferred to a 50 mL conical vial containing 45 mL of DMEM<sup>-</sup> and 10% FBS. The solution was vortexed and 8 mL was added to six 10 cm dishes. Cells were allowed to grow to 60% confluency over 24 hours.

### **Nystatin Treatments**

Nystatin treatments were used for half of the 60% confluent dishes. Nystatin treatments with a concentration of 60 µg/µl, were added to 3 mL of DMEM<sup>-</sup> media in attempts to reduce the complete absence of cholesterol and caveolae within the plasma membrane. Nystatin treatments

were for 30 minutes and conditions were set at 37° C, 5% CO<sub>2</sub>, and 90% humidity. Normal DMEM<sup>-</sup> media was added to the three untreated 10 cm dishes as a control.

### **MCH Treatment**

Once cells were treated, MCH treatments were carried out for 10 minutes and 30 minutes. In 8 mL of DMEM+10% FBS media, 1 μM of MCH was added. Old media within the 10 cm dishes was aspirated off and MCH solution was added for desired amount of time.

### **Homogenate Preparation**

After 30 minutes of incubation, media from treated and untreated dishes was aspirated off. All 6 dishes were washed twice with 5 mL of cold phosphate buffered saline (PBS). PBS was made by adding 80 g NaCl, 2 g KCl, 14.4 g Na<sub>2</sub>HPO<sub>4</sub>, 2.4 g KH<sub>2</sub>PO<sub>4</sub> to 800 mL of ddH<sub>2</sub>O. Once the second wash was aspirated off of treated and untreated dishes, 2 mL of 500 mM sodium carbonate (pH 11) was added to 1:1000 protease inhibitor (Thermo Scientific) to create a protease/phosphatase inhibitor cocktail. The mixture was vortexed and 1 mL was added to 1 dish of nystatin-treated cells and the remaining 1 mL was added to 1 dish of the untreated cells. Using a cell scraper, the cells were removed from the bottom of the both the treated and untreated dish and became suspended in the media. The media was then transferred to the next dish that contained the same type of cells of the first dish. After a second scrape, the media was added to the final dish that produced a concentrated amount of treated and untreated cells. Treated and untreated cell lysates were added to separate Dounce homogenizers on ice. Each was homogenized for 10 strokes and then sat for 2 minutes before 2 more homogenizations were carried out with 2 minute in between. All above procedures were performed on ice.

## **Sucrose Gradient Generation**

In order to separate the lysates based upon density, the homogenate was loaded into a sucrose gradient that was of differing densities. Post homogenation, 2 mL of treated and untreated lysates were loaded into separate ultracentrifugation tubes with 1 mL of 90% sucrose (9.9g of Sucrose and 11 mL of ddH<sub>2</sub>O). The ultracentrifugation tube was then vortexed to make 45% sucrose solution (1mL of 90% sucrose and 2 mL of homogenate). After vortexing, 4 mL of 35% sucrose was added to the tube drop wise as to not disturb the denser layer. To bring the gradient up to 12 mL, 4-5 mL of 5% sucrose was added drop wise to the tube. 35% and 5% solutions were made in an MBS buffer made by dissolving 97.6 g MES (free acid) in 800 mL of ddH<sub>2</sub>O, bringing up the volume to 1 L with ddH<sub>2</sub>O. pH was adjusted for solution using 10 N NAOH. Both tubes were then weighed in order to balance them as to prevent anomalies during ultracentrifugation.

## **Ultracentrifugation**

Treated and untreated sucrose gradients were placed into titanium tube holders and attached to a SW-41 swinging bucket rotor. The bucket was attached to the ultracentrifuge and was run at 39,000 rpm for 18 hours at 4°C.

## **Fraction Collection and Preparation**

Post ultracentrifugation, (12) 1mL fractions were removed from the tubes starting from the top of the gradient and moving towards the bottom. Fractions were stored in the freezer overnight. After 24 hours, 25 uL of 5X Lamanelli sample buffer was added to each fraction. Lamanelli sample buffer was made by adding 1.5 g SDS to 3.75 ml 1M Tris (pH 6.8)

, 0.075 g bromophenol blue, 480  $\mu$ l of BME, 7.5 mL of glycerol, and 7.5 mL of H<sub>2</sub>O. A 100  $\mu$ L of each fraction was removed and placed in a boiling water bath for 2 minutes. Fractions were then spun in a microcentrifuge for 2 minutes at 13,000 rpm and 4 °C.

### **Bradford Protein Analysis**

Fractions were then placed in a 96 well plate for confirmation that protein existed. The first two rows of wells were filled with 20  $\mu$ L of Bovine Serum Albumin (BSA) standard followed by two rows with 20  $\mu$ L of untreated fractions and two rows of 20  $\mu$ L treated fractions. In addition, 200  $\mu$ L of 1X Bradford reagent was added to each well. Bradford reagent was made by adding 100 mg Coomassie blue to 50 mL of 90% ethanol, 100 ml of 85% phosphoric acid along with 50 mL of ddH<sub>2</sub>O. The 96 well plate was read 595nm using a Synergy 1 plate reader.

### **Gel Electrophoresis and Wet Transfer**

A Sodium Dodecyl Sulfate Polyacrylamide Gel Electrophoresis (SDS/PAGE) apparatus was prepared. In order to generate two 75mm 12% gels, a 12% running solution and a 4% stacking solution were made. For the 12% running buffer, 3.0 mL of 40% BIS Acrylamide along with 2.5 mL of 4X TrisCl/SDS (pH 8.8), 33  $\mu$ L of 10% APS and 4.5 mL of ddH<sub>2</sub>O were mixed. The stacking buffer was made by combining 0.5 mL of 40% BIS Acrylamide, 1.25 mL of 4X TrisCL/SDS (pH 6.8), 25  $\mu$ L of 10% APS and 3.20 mL of ddH<sub>2</sub>O. The addition of 6.6  $\mu$ L of Tetramethylethylenediamine (TEMED) to the running solution polymerized the gel after 30 minutes of being loaded into the constructed apparatus. After polymerization, 6  $\mu$ L of TEMED was added to the stacking solution and was added on top of the polymerized running solution within the apparatus. Plastic spacers were then inserted to create wells within the gel. After a subsequent 30 minutes, 40  $\mu$ L of the prepared samples were loaded into 12 separate wells along with 5  $\mu$ L of a protein ladder (BIO-RAD) in 2 separate gels, one for untreated one for nystatin

treated. The SDS/PAGE ran at 150 V for 110 minutes. Post SDS/PAGE, both gels were placed between separate filter paper and a nitrocellulose membrane that were then placed in a transfer buffer for 15 minutes. The transfer buffer was prepared by adding 11.6 g glycine, 23.2 g Tris Base, 1.48 g SDS, and 800 mL methanol in 1 L of water which was brought to 5 L with the addition of 4 L of water. The wet transfer apparatus ran for 45 minutes at 350 mA.

### **Western Blot Analysis**

After the completion of the wet transfer, both nitrocellulose membranes were blocked in 10 mL of 5% dry milk made from 1 g of powdered milk and 20 mL of Tris-Buffered Saline-Tween (TBS-T) for 1 hour. TBS-T was made through the addition of 250  $\mu$ l of TWEEN to 200 mM Tris-Cl, and 1.4 M NaCl. Post blocking, both membranes were treated with a 1:1000 dilution of Rabbit Anti-Cavelolin-1 Antibody (BioRad). Membranes were stored in cold room 4°C overnight. The primary antibody was removed through three 10 minute washes of the membranes with 5 mL TBS-T preparing membranes for the secondary antibody treatment. The secondary antibody used was a 1:10,000 dilution of Goat Anti-Rabbit Antibody (BioRad). The secondary antibody procedure lasted 45 minutes followed by another three 10 minute washes with 5 mL TBS-T.

### **Chemiluminescent and Development**

Membranes were prepared for fixation and development according to the ECL kit protocol provided by Thermo Scientific. Membranes were transferred to a dark room where development and fixation of the proteins was carried out and a film developed on KODAK film.



## **RESULTS**

### **Designing a Strategy to Disrupt Caveolae**

MCH has been shown to play an integral role in regulating energy homeostasis. Studies have shown that MCH knockout mice contain a lean phenotype indicating MCH's role in food consumption. MCH can bind to MCHR-1 or and internalize via clathrin or caveolae mediated endocytosis (Razani et al. 2002; Cook, Delorme-Axford, and Robinson 2008). Further, MCHR-1 has been shown to activate multiple signaling pathways through the activation of  $G_q$ ,  $G_i$ , and  $G_0$  proteins. In addition MCHR-1 has been shown to co localize with caveolae lipid rafts within the plasma membrane (Moden et al. 2013).

To further understand how MCHR-1 disruption can lead to decreased internalization of MCH, caveolae lipid rafts must be disrupted. The antibiotic Nystatin has been shown to be a viable cholesterol inhibitor that can be used to disrupt co-localization of caveolae and MCHR-1. A recent study by Hussain and colleagues utilized nystatin to disrupt the plasma membrane of host cells in attempts to disrupt the entry of the human enterovirus (HEV71). Reduction in infection indicated that nystatin treatments did indeed disrupt functional receptor localization to the plasma membrane providing evidence that nystatin was an effective pharmacological tool (Hussain et al. 2011).

With previous research by Hussain and colleagues confirming its validity, nystatin, was used in attempts to sequester caveole and disrupt its co-localization with MHCR-1. Confluent BHK-570 cells were treated with Nystatin over a 30 minute period. Cell lysis and ultracentrifugation were used to separate caveolae from the different parts of the cell.

The main structural component of the lipid raft caveolae is a protein known as caveolin-1. Consequently, a protein assay known as a Bradford analysis was used to show 1) The presence

or reduction of caveolin-1 within the cell 2) the determination of how much total protein was present in each fraction.

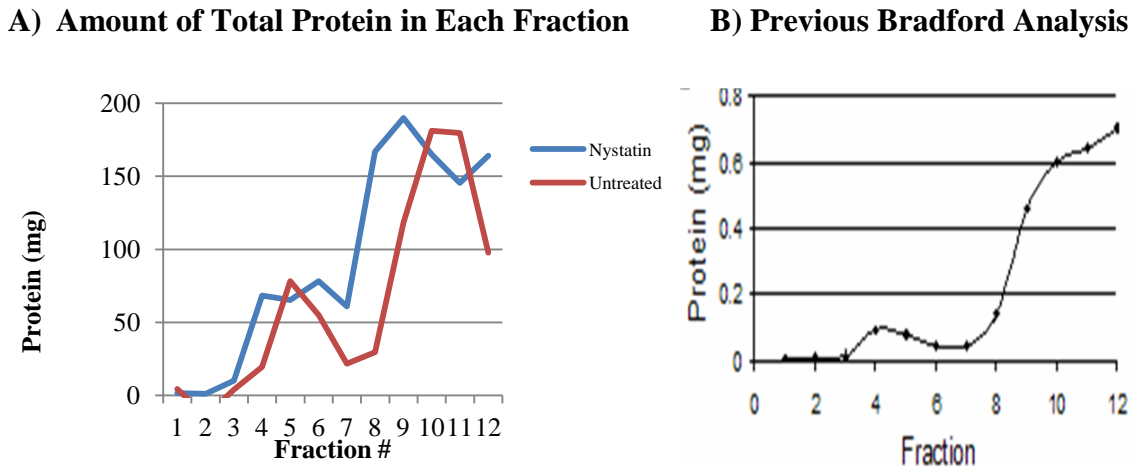


**Figure 1: A) Bradford Analysis of Untreated and Treated Cells indicates a shift in protein fraction amount.** BHK-570 cells were either treated with 60 ul/ug of Nystatin for 30 minutes or left untreated. Cell lysis and ultracentrifugation were completed followed by a Bradford analysis. Nystatin treatments show a shift in protein amount, specifically in fractions # 4, 5, 6, and 7. **B) Previous Bradford Analysis of Untreated BHK-570 Cells performed by (Cook et al. 2008)** indicates that there is indeed an increase of total protein content within fractions #4,5,6.

When compared to studies carried out by Cook and colleagues, total protein concentration within the fractions is normal for untreated cells. As seen in Fig 1A. there was a 12 mg increase in protein presence from fraction 4 compared to fraction 5 in untreated cells. Further, higher protein amounts were seen in fractions 10-12 for both untreated and nystatin due to the high density of most proteins within the cell. Both dishes were assumed to have the same total protein content as they were grown under the same conditions for equal amount of time. Being able to reproduce already published results (Fig 1B) increased the validity of this data and allowed for secondary experiments to proceed. It is important to note that Bradford analysis of the separated sucrose gradients yielded total protein concentration, not just the presence of the caveolae protein.

## Percent of Total Protein in Each Fraction

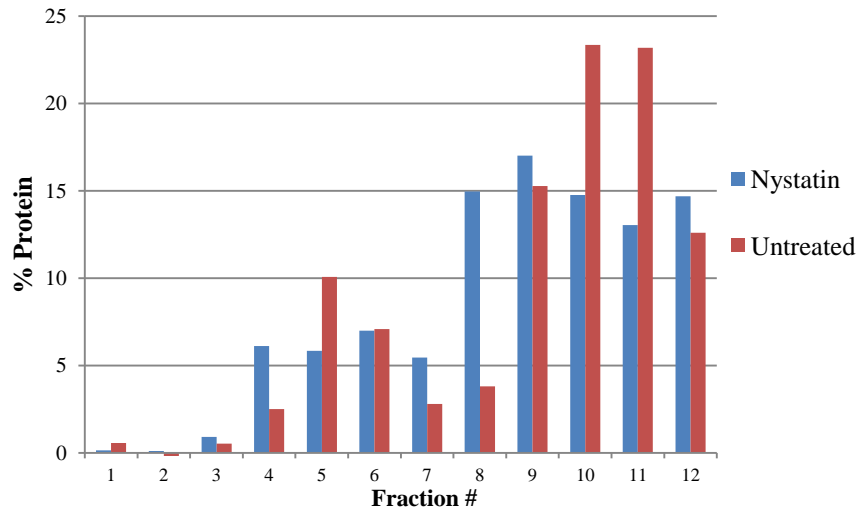


**Figure 2: Bradford Analysis of Untreated and Treated Cells indicates a change in the percentage of protein within fractions.** BHK570 cells were either treated with Nystatin for 30 minutes or left untreated. Cell lysis and ultracentrifugation led to fraction collection and subsequent Bradford analysis. Analysis revealed that percent of protein within certain fractions was altered. Again, fractions # 4, 5, 6, and 7 were particularly affected.

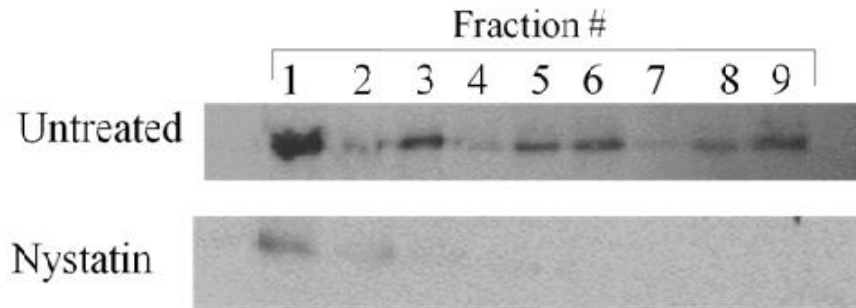
Through Bradford analysis, the percentage of protein within each fraction was able to be calculated. This calculation was necessary to show that as expected, nystatin shifted protein content into higher fractions. As seen in Fig 2., the increase in protein content in fractions 6 and 7 was a direct result of nystatin as its presence within the plasma membrane made the proteins more dense resulting in a shift to higher fractions. Subsequent analysis of the Bradford data indicated that fraction 4 experienced a 50% increase in protein content after nystatin treatments while fraction 5 had a 50% decrease in protein. Fraction 6 remained relatively unchanged while fraction 7 experienced a 35% increase in protein concentration after nystatin treatments. Again Bradford analysis only calculated total protein percentage and not just the percentage of caveolae within the fractions.

Caveolae invaginations within the plasma membrane are coated with a marker protein known as caveolin-1 (CAV-1). Early endosomes of the caveolae mediated endocytic pathway are coated with CAV-1 indicating, the strong relationship between caveolae and CAV-1.

Also associated with caveolae is cholesterol that makes the lipid rafts highly stiff. Increased rigidity can potentiate the signals caused by hormones either through endocytosis or secondary signaling. When cholesterol is absent, membrane fluidity increases, inhibiting the presence of viable signaling mechanisms which may decrease the effects of hormones. Cholesterol sequestration is a direct target of certain antibiotics in attempts to disrupt plasma membrane formation and signaling. Nystatin is an antibiotic that acts through cholesterol sequestration that produces abnormal plasma membrane behavior that leads to cell death in bacteria (Lampan et al. 1962).

When administered in small doses to BHK-570 cells, nystatin can be a potent inhibitor of normal cholesterol formation within the plasma membrane (Hussain et al. 2011). As a result of nystatin treatments, cholesterol enriched caveole regions decrease reducing the presence of CAV-1. Consequently, western blot analysis that indicates the presence of CAV-1 through use of antibodies should show a decrease in CAV-1 in nystatin treated cells.

**A) Western Blot Analysis of Untreated and Nystatin Treated BHK-570 Cells B)**



**B) Previous Research : Western Blot Analysis of Untreated BHK-570 Cells**

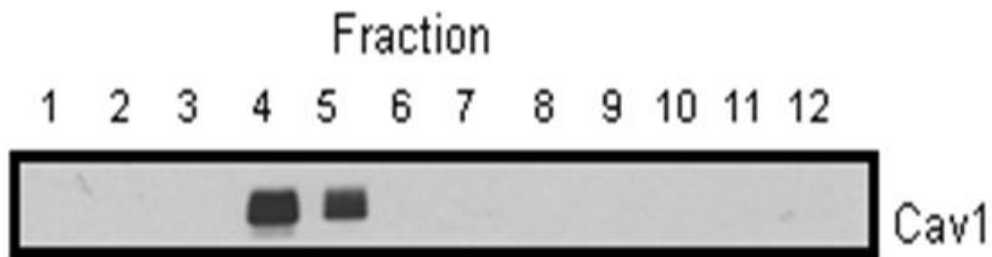


**Figure 3: A) Western Blot analysis reveals that CAV-1 is reduced within Nystatin treated BHK-570 cells.** Fractions of both untreated and treated cells were subjected to SDS/PAGE. After completion, gel was subjected to wet transfer process that moved protein from gel to nitrocellulose membrane. Membrane was blocked and then treated with a 1:5000 dilution of 1° Rabbit Anticaveolin-1 antibody and allowed to treat overnight. Membrane was then treated with 2° Goat Antirabbit antibody and subjected to chemiluminescence and development and fixation in order to make the CAV-1 bands visible. Picture presented shows bands present at 25 kDA. **B) Western Blot analysis of BHK-570 cells blocked for CAV-1** conducted by (Cook et al. 2008) illustrated dark bands within fractions 4 and 5 at the 25 kDA marker indicative of CAV-1.

Western blot analysis was carried out after SDS/PAGE and antibody treatments. The use of a chemiluminescent kit illustrated the presence of CAV-1 within fractions. Fig 3.A indicated dark banding within fractions 1, 5 and 6 of the untreated cells while light banding occurred in fraction 1 in the treated cells. The absence of banding in other fractions is indicative of the loss or shift in caveolae due to nystatin. Unlike the Bradford analysis, western blotting allowed for the identification of one specific protein instead of the total content within fractions. For this study, comparing Bradford analysis in Fig 1A data to western blot results (Fig 3A) shows that protein was present within all fractions but CAV-1 was only in certain areas of the sucrose

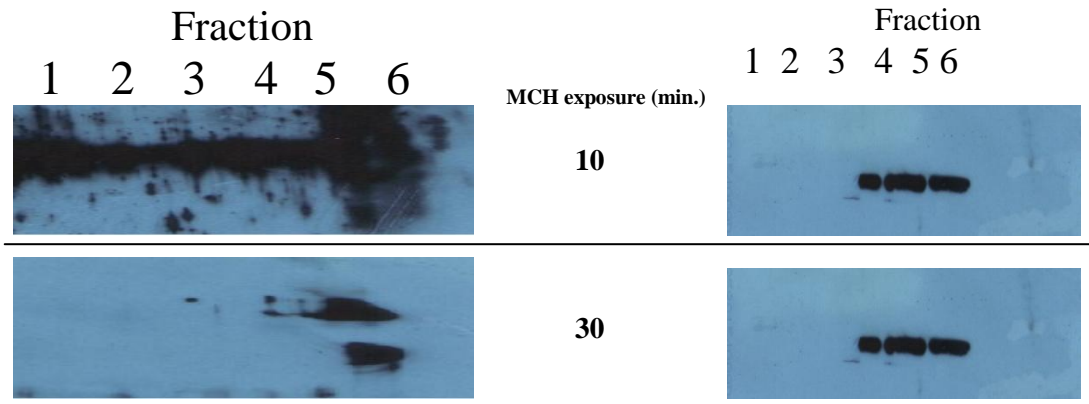
gradient. Results of this study were also compared to previous research done by Cook et al. 2008 in order to increase its validity as a successful western blot.

### **MCH treatment after Caveolae Disruption**

After a standard protocol produced adequate caveolae disruption, timed MCH treatments were carried out in order to investigate if MCH internalization was disrupted. Previous research has indicated that MCHR-1 localization within caveole membranes may play a role in signal internalization or that internalization is completely independent of this pathway (Moden et al. 2013). In order to test this postulate it is crucial to identify MCHR-1 co localization with caveolae and then determine whether after timed MCH treatments, there is a significant decrease of MCHR-1 on the plasma membrane. Because BHK-570 cells lack an endogenous MCHR-1, transfection of a VSVg-MCHR-1 was carried out. After cells were grown to confluence, both untreated and treated cells were subjected to MCH treatments of 0, 10, and 30 minutes. Subsequent ultracentrifugation, SDS/PAGE, and western blot analysis illustrated the effect of MCH treatments on MCHR-1 and caveolae presence within the fractions.

**A) Isolated Fractions: VSVG-MCHR1**

**B) Isolated Fractions: CAV-1**



**C) Previous Research**

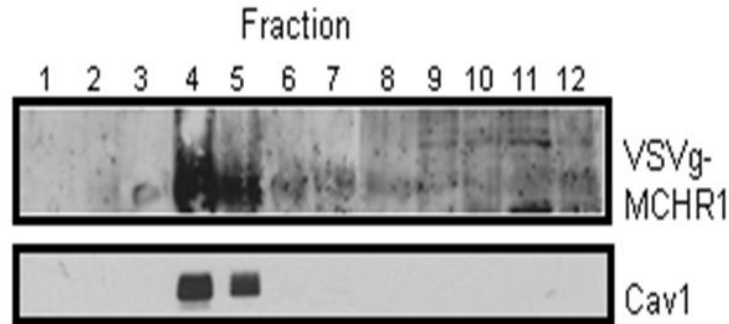


**Fig 4: A) Isolated Fractions of Untreated Cells blocked for VSVG-MCHR-1** indicated a heavy presence of VSVg-MCHR-1 receptor within fractions 4 and 5. At 10 minutes, of MCH exposure, VSVg-MCHR-1 localizes to fractions 4 and 5. The majority of MCH receptor localizes to fraction 4 at 0 minutes of exposure (data not shown) with a molecular weight up shift after 10 minutes, illustrated by the dark banding in fraction 5. After 30 minutes, VSVg-MCHR-1 is still present within fraction 5 indicating that there is still an increase in molecular weight. Banding was present at 72-55 kDa. **B) Isolated Fractions of Untreated Cells blocked for CAV-1** indicated an increased presence of CAV-1 within the fractions that were previously shown to show VSVg-MCHR-1. Banding occurred at 25 kDa. **C) Previous Research has shown that VSVg-MCHR-1 is primarily associated with fractions 4 and 5.** Cook et al. 2008 illustrated the presence of both VSVg-MCHR-1 and CAV-1 within fractions 4 and 5.

Western blot analysis revealed that CAV-1 and VSVg-MCHR-1 are highly co-localized showing up in the same fractions during timed MCH treatments. CAV-1 is present throughout MCH exposure and its co-localization with MCHR-1 is evident in fractions 4 and 5 at 0-minutes (data not shown), in fractions 4,5,and 6 at 10-minutes and in fraction 5 at 30-minutes MCH exposure. The previous research conducted by Cook et al. 2008 served as a comparison in order to validate the success of the experiment (Fig 4C). Nonetheless, all blots presented are of

untreated BHK-570 cells. Data collected on cells treated with nystatin are hard to interpret due to a high amount of background within the developed pictures. It is the goal of future research to prevent this interference and present reliable data that describes the relationship between VSVg-MCHR-1 and MCH co-localization and internalization.



## **DISCUSSION**

*Sucrose Gradient Generation and Western Blot Analysis procedures were mastered correctly*

It was crucial for this study to adequately produce sucrose gradients and western blot analysis that quantified protein content as well as the presence of caveolae. The sucrose gradient was considered a success because the untreated cells expressed about the same curve as Cook *et al.* had previously shown. Previous research by Cook and colleague has also indicated that caveolae and lipid rafts tend to separate within fractions 4, 5, and 6 of the sucrose gradient based upon their molecular weight (Cook *et al.* 2008). This information allowed for the further investigation of fractions 4, 5, and 6 throughout the study and when these regions are compared between untreated and treated cells, there seems to be a difference.

Treated cells showed a shift in protein content near fractions 4, 5 and 6 which was expected as the presence of nystatin altered the density and formation of the lipid rafts. Alteration was shown in Fig 1A by a plateau between fractions 4, 5 and 6. When compared to the untreated cells, which only show an increase in protein content at fraction 5, there seems to be some disruption within the lipid raft region due to the presence of nystatin. Within fractions 4-6 of nystatin treated cells there is a 62% increase in protein content from untreated cells (Fig 2). Results from the Bradford analysis indicated that protein within the nystatin treated cells may 1) be more abundant because of an increased number of cells when lysed or 2) The presence of nystatin caused a shift of protein in the lipid raft region due to its ability to sequester cholesterol. Subsequent western blot analysis was a success as the presence of caveolae was clearly shown by dark banding in the 25 kDa region of the untreated cells in fractions 5 and 6 (Fig 3A).

Despite the mastery of these techniques, challenges surrounded this portion of the study. In order to generate a polymerized gel that could separate the protein based upon weight the

exact concentrations of the running and stacking solutions had to be used. At times gels were too thin due to the lack of TEMED added. Thinner gels resulted in the loss of caveolae as it travelled too far down the gel and was lost before transfer. Therefore, when an adequate gel was produced the exact amount of TEMED was recorded and served as the standard for the remainder of the study.

Cell number also posed a challenge for this study. In order to generate enough cells to express cav-1 at detectable levels, BHK-570 had to be grown for 48 hours on 10 cm culture dishes. The issue arose when the cells were lysed and there were no prior controls used to determine if both the untreated and the treated had the same number of cells. Increased cells within either the untreated or treated may have contributed to an increased expression of caveolae. Increased expression of caveolae because of a greater cell number limits the conclusions that support the efficacy of nystatin treatment. Future studies will include use of a hemocytometer, a device that is used to calculate the exact number of cells (Van der Linden et al. 2014). Knowing that both the untreated and treated experiments contain the same number of cells will make future conclusions surrounding the effectiveness of pharmacological membrane disruptors much stronger.

#### *Cholesterol depletion with nystatin alters the formation and presence of caveolae*

In bacteria, nystatin has been shown to disrupt the plasma membrane and lead to cell death (Lampen et al. 1962). Within BHK-570 cells, however, nystatin is used to deplete cholesterol which effectively disassembles caveolae lipid rafts. If MCHR-1 were enriched in caveolae, lipid raft disruption would subsequently be expected to alter signaling. A decrease in caveolae was shown by blocking for caveolin-1 (cav-1), a structural protein of caveolae. According to Fig 3A, 1.5 hour exposure to 60 µg/µl of nystatin can effectively deplete the

plasma membrane of caveolae. The absence of dark banding in fractions 5 and 6 that were present in untreated cells, indicate that nystatin treatments can effectively decrease the amount of caveolae.

Previous research has shown that antibiotic treatments can severely deform cellular structure leading to a decrease in proper plasma membrane formation (Cook et al. 2008). The lack of proper formation of lipid rafts instead of complete caveole destruction seems to be the best conclusion of this study. Even though cav-1 is not present within the western blot, the Bradford analysis shows a strong presence of protein in nystatin treated cells. These results are indicative of cav-1 being present but in smaller amounts and spread throughout fractions 4, 5 and 6. According to Fig 2., there is approximately four times the amount of protein within fraction 5 of the untreated cells when compared to fraction 4. Coupled with the blot analysis shown in Fig 3.A. this spike is indicative of cav-1 present in fraction 5. When examining the nystatin treated cells, fraction 5 contains 50% less protein (Fig 2.) which may account for the light band seen on the blot (Fig 3.A). Nevertheless, the presence of nystatin is shown to alter the localization of cav-1 to caveolae fractions on sucrose gradients.

*MCHR-1 localization to caveolin-1 enriched fractions is independent of 0.250- $\mu$ M MCH treatment at 10 minutes with equal protein content*

Exposure to 1  $\mu$ M MCH appeared to have no effect on receptor localization to caveolin-1 fractions within 10 minutes or 30 minutes. Fig 4 A, B indicates the presence of a properly expressed VSVg-MCHR-1 within BHK-570 cells along with its co-localization to cav-1 and its presence in the 30 minute MCH treatment time. Unfortunately, data for 0- minutes could not be shown due to increased interference on the blot, like the 10-minute exposure time, both MCHR-1 and cav-1 remained localized to fractions 4 and 5. A hypothesized explanation for this data is

that the receptor has not yet undergone internalization from the plasma membrane and remains within lipid rafts at 10-minutes. To test this, a longer time course of hormone treatment was carried out.

After 30 minutes of exposure, MCHR-1 seemed to localize primarily within fraction 5 indicating that an up shift in molecular weight of MCHR-1 (Fig 4A). This up shift could be due to MCH/MCHR-1 interaction as well as the preparation for caveolar mediated internalization which is initiated by post translational modifications of MCHR-1 (Saito, Hamamoto, and Kobayashi 2013). As a result, prolonged hormone treatments may show that internalization via caveolae does occur.

Previous research Moden *et al.* indicates that MCHR-1 and cav-1 do co-localize and prolonged hormone treatments produce MCH internalization. Moden *et al.* reports that after 30 minutes of MCH treatment, 62% of surface MCHR-1 was internalized. Whether this process is caveolae or clathrin mediated remains to be determined suggesting that even if caveolae was depleted there still will be receptor internalization (Moden et al. 2013). Consequently, no conclusions can be made regarding the effect of cholesterol depletion, and subsequent destruction of caveolae on MCHR-1 internalization.

The lack of a conclusion within this study is also due in part to the lack of data presented on nystatin treated cells. The MCH treatments performed were done on untreated cells in attempts to establish a viable protocol for future studies on nystatin cells. It is the hope that this project will pursue hormonal studies on treated cells in order to establish a clear relationship between MCHR-1 caveolae co-localization and MCH internalization.

Other technical errors prevented strong conclusions to be stated. Some procedures presented were only replicated twice bringing into question their validity as normally accepted

studies can be replicated numerous times by the primary investigator or other research institutions. In addition, fraction separation could have been altered within both experiments as pipetteing techniques for this type of collection is difficult to control.

### *Future Directions*

There are several potentially promising directions that this project could take. First, the use of siRNA to delete cav-1 solely rather than pharmacological cholesterol depletion can be carried out. Oh and colleagues have previously shown that cav-1 siRNA has severely inhibited the proper formation of caveolae enriched regions within the plasma membrane. Decrease in these regions could decrease the co-localization between caveolae and MCHR-1 (Oh and Schnitzer 2001). This genetic alteration, however, could have ill advised side effects on the cell that may inhibit other functioning pathways. Second, other pathways that are affected by MCH can be investigated before and after caveolae depletion. These pathways include MAPK1 which regulates secondary signaling within the cell that can lead to desensitization.

Third, the use of an endogenous cell line, such as the 3T3L-1 pre-adipocyte or differentiated adipocyte, is critical for assessing the functional role of MCHR-1 in caveolae. Fourth, the role of MCHR-1 may also be affected by phosphorylation. As indicated by data there is an upshift in molecular weight during 30 minute treatment time (Fig 4A). We hypothesize as do others, that this molecular up shift could have been caused by the phosphorylation of MCHR-1 after MCH binding. Saito and colleagues report that the receptor phosphorylation and subsequent binding of  $\beta$ -arrestin prevent consequent interactions of the receptors with G-proteins, thereby effectively terminating the G-protein-mediated signaling and initiating the endocytic process (Saito, Hamamoto, and Kobayashi 2013). This phosphorylation activity can be an effective target for future investigations and treatments concerning MCH. If MCHR-1 can be

constitutively phosphorylated, desensitization could lead to a viable treatment option in combating the obesity epidemic.

## Refereneeces

- Bjursell, M. 2006. “Melanin-Concentrating Hormone Receptor 1 Deficiency Increases Insulin Sensitivity in Obese Leptin-Deficient Mice Without Affecting Body Weight.” *Diabetes* 55 (3) (March 1): 725–733. doi:10.2337/diabetes.55.03.06.db05-1302.
- Bradley, R L, E G Kokkotou, E Maratos-Flier, and B Cheatham. 2000. “Melanin-concentrating hormone regulates leptin synthesis and secretion in rat adipocytes.” *Diabetes* 49 (7) (July): 1073–1077.
- Cook, Laurie B., Elizabeth B. Delorme-Axford, and Kelsi Robinson. 2008. “Caveolae as Potential Mediators of MCH-signaling Pathways.” *Biochemical and Biophysical Research Communications* 375 (4) (October): 592–595. doi:10.1016/j.bbrc.2008.08.038.
- Delporte, Christine. 2012. “Recent Advances in Potential Clinical Application of Ghrelin in Obesity.” *Journal of Obesity* 2012: 1–8. doi:10.1155/2012/535624.
- Derksen, D. J. 2013. “The Affordable Care Act: Unprecedented Opportunities for Family Physicians and Public Health.” *The Annals of Family Medicine* 11 (5) (September 1): 400–402. doi:10.1370/afm.1569.
- Ferguson, S S. 2001. “Evolving concepts in G protein-coupled receptor endocytosis: the role in receptor desensitization and signaling.” *Pharmacological reviews* 53 (1) (March): 1–24.
- Finkelstein, E. A., J. G. Trogon, J. W. Cohen, and W. Dietz. 2009. “Annual Medical Spending Attributable To Obesity: Payer-And Service-Specific Estimates.” *Health Affairs* 28 (5) (September 1): w822–w831. doi:10.1377/hlthaff.28.5.w822.
- Gehlert, D. R., K. Rasmussen, J. Shaw, X. Li, P. Ardayfio, L. Craft, T. Coskun, H. Y. Zhang, Y. Chen, and J. M. Witkin. 2009. “Preclinical Evaluation of Melanin-Concentrating Hormone Receptor 1 Antagonism for the Treatment of Obesity and Depression.” *Journal*

- of Pharmacology and Experimental Therapeutics* 329 (2) (May 1): 429–438.  
doi:10.1124/jpet.108.143362.
- Harwood, H. James. 2012. “The Adipocyte as an Endocrine Organ in the Regulation of Metabolic Homeostasis.” *Neuropharmacology* 63 (1) (July): 57–75.  
doi:10.1016/j.neuropharm.2011.12.010.
- Hassani, O. K., M. G. Lee, and B. E. Jones. 2009. “Melanin-concentrating Hormone Neurons Discharge in a Reciprocal Manner to Orexin Neurons Across the Sleep-wake Cycle.” *Proceedings of the National Academy of Sciences* 106 (7) (February 17): 2418–2422.  
doi:10.1073/pnas.0811400106.
- Hussain, K. M., K. L. J. Leong, M. M.-L. Ng, and J. J. H. Chu. 2011. “The Essential Role of Clathrin-mediated Endocytosis in the Infectious Entry of Human Enterovirus 71.” *Journal of Biological Chemistry* 286 (1) (January 7): 309–321.  
doi:10.1074/jbc.M110.168468.
- Kopelman, P G. 2000. “Obesity as a medical problem.” *Nature* 404 (6778) (April 6): 635–643.  
doi:10.1038/35007508.
- Lampen, J O, P M Arnow, Z Borowska, and A I Laskin. 1962. “Location and role of sterol at nystatin-binding sites.” *Journal of bacteriology* 84 (December): 1152–1160.
- Van der Linden, Noreen, Lieke J J Klinkenberg, Steven J R Meex, Erik A M Beckers, Norbert C J de Wit, and Lenneke Prinzen. 2014. “Immature platelet fraction measured on the Sysmex XN hemocytometer predicts thrombopoietic recovery after autologous stem cell transplantation.” *European journal of haematology* (March 24). doi:10.1111/ejh.12319.
- Moden, Jay I., Katrina Haude, Robert Carroll, Andrew Goodspeed, and Laurie B. Cook. 2013. “Analyzing the Role of Receptor Internalization in the Regulation of Melanin-



- Concentrating Hormone Signaling.” *International Journal of Endocrinology* 2013: 1–10.  
doi:10.1155/2013/143052.
- Ogden, Cynthia L., Margaret D. Carroll, Brian K. Kit, and Katherine M. Flegal. 2014.  
“Prevalence of Childhood and Adult Obesity in the United States, 2011-2012.” *JAMA*  
311 (8) (February 26): 806. doi:10.1001/jama.2014.732.
- Oh, P, and J E Schnitzer. 2001. “Segregation of heterotrimeric G proteins in cell surface  
microdomains. G(q) binds caveolin to concentrate in caveolae, whereas G(i) and G(s)  
target lipid rafts by default.” *Molecular biology of the cell* 12 (3) (March): 685–698.
- Pissios, Pavlos, and Eleftheria Maratos-Flier. 2003. “Melanin-concentrating hormone: from fish  
skin to skinny mammals.” *Trends in endocrinology and metabolism: TEM* 14 (5) (July):  
243–248.
- Razani, Babak, Terry P Combs, Xiao Bo Wang, Philippe G Frank, David S Park, Robert G  
Russell, Maomi Li, et al. 2002. “Caveolin-1-deficient mice are lean, resistant to diet-  
induced obesity, and show hypertriglyceridemia with adipocyte abnormalities.” *The  
Journal of biological chemistry* 277 (10) (March 8): 8635–8647.  
doi:10.1074/jbc.M110970200.
- Saito, Yumiko, Akie Hamamoto, and Yuki Kobayashi. 2013. “Regulated Control of Melanin-  
Concentrating Hormone Receptor 1 through Posttranslational Modifications.” *Frontiers  
in endocrinology* 4: 154. doi:10.3389/fendo.2013.00154.
- Sam, Amir H., Rachel C. Troke, Tricia M. Tan, and Gavin A. Bewick. 2012. “The Role of the  
Gut/brain Axis in Modulating Food Intake.” *Neuropharmacology* 63 (1) (July): 46–56.  
doi:10.1016/j.neuropharm.2011.10.008.
- Simons, K. 2001. “Lipid Rafts and Signal Transduction.”

Vemmos, K., G. Ntaios, K. Spengos, P. Savvari, A. Vemmou, T. Pappa, E. Manios, G.

Georgiopoulos, and M. Alevizaki. 2011. "Association Between Obesity and Mortality After Acute First-Ever Stroke: The Obesity-Stroke Paradox." *Stroke* 42 (1) (January 1): 30–36. doi:10.1161/STROKEAHA.110.593434.

Williams, G, J A Harrold, and D J Cutler. 2000. "The hypothalamus and the regulation of energy homeostasis: lifting the lid on a black box." *The Proceedings of the Nutrition Society* 59 (3) (August): 385–396.

Woods, S C, R J Seeley, D Porte Jr, and M W Schwartz. 1998. "Signals that regulate food intake and energy homeostasis." *Science (New York, N.Y.)* 280 (5368) (May 29): 1378–1383.